

### 0.0.1 The Signal Separation Challenge

In the PICO frequency range there are Galactic and Extra-Galactic sources of emission. Galactic emissions are due to free-free, synchrotron, and dust, which arise respectively from photon emission in free electron-proton scattering, free electrons spiraling around Galactic magnetic field lines, and from  $\sim 20$  K elongated interstellar dust grains partially aligned with the local magnetic field. Free-free emission is expected to have negligible polarization. The emission from synchrotron and dust are linearly polarized, and has both  $E$  and  $B$  components (Fig. 1). Extra-Galactic sources of emission include the CMB, which has both  $E$  and  $B$ -modes, and point sources of whose polarization level and type are not well constrained. The task of ‘separating the signal to its components’ (sometimes shortened to ‘component separation’) is to decompose the detected signal to its constituent sources. The required precision of signal separation is determined by the requirement to detect or set an upper limit on the inflationary  $B$ -mode, which is the faintest among PICO’s targeted signals. In that context, the terms ‘foreground separation’ and ‘foreground cleaning’ are used as equivalents to ‘signal separation’.

Galactic emission dominates the sky’s polarized intensity on large angular scales ( $\ell \lesssim 10$ ), it dominates the cosmological  $B$ -modes signals for  $\ell \lesssim 150$  for all allowed levels of  $r$ , and it is expected to be significant even at  $\ell \simeq 1000$ , posing challenge for reconstructing the  $B$ -mode signal from lensing. This is illustrated in Figs. ?? and 1, which show Galactic emission power spectra calculated for the cleanest – that is, the least Galactic-emission-contaminated – 60% of the sky. But even in small patches of the sky, far from the Galactic plane and with the least foreground contamination, Galactic emission levels are substantial relative to an inflationary signal of  $r \sim 0.01$  and overwhelm it for  $r \lesssim 0.001$  [? ]. Separating the cosmological and Galactic emission signals is *the* primary challenge facing any next-decade experiment attempting to reach these levels of constraints on  $r$ , along with control of systematic uncertainties.

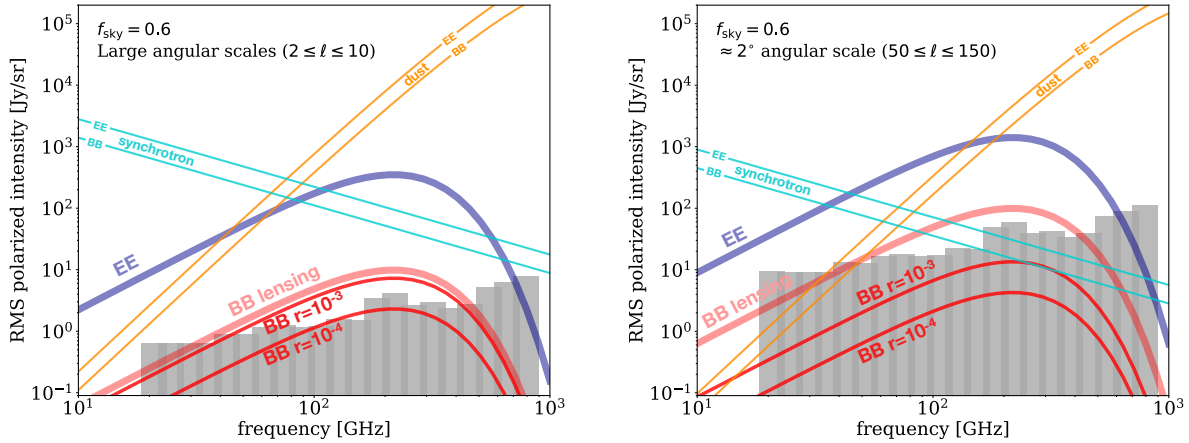


Figure 0.1: Polarization  $BB$  spectra of Galactic synchrotron and dust, compared to CMB polarization  $EE$  and  $BB$  spectra of different origins for two values of  $r$  and for two ranges of angular scales: large-scale,  $\ell \leq 10$ , corresponding to the reionization peak (left panel); and intermediate  $50 \leq \ell \leq 150$ , corresponding to the recombination peak (right panel). Data from *Planck* indicate that for Galactic emission the level of  $E$ -mode is approximately twice that of  $B$  [? ]. The PICO baseline noise (grey bands) is low compared to the Galactic emission components, and thus they will be measured with high **SNR!** in many frequency bands.

Foreground separation is challenging because the spatial power spectra and frequency spectra of the foregrounds are not known to sufficient accuracy anywhere across the sky. To a first approximation, the spectrum of synchrotron emission is a power law  $I_{\text{sync}} \propto \nu^\alpha$ , with  $\alpha \simeq -1$ . The spectrum of dust emission is  $I_{\text{dust}} \propto \nu^\beta B_\nu(T_{\text{dust}})$ , where  $\beta \simeq 1.6$ ,  $T_{\text{dust}} \simeq 20$  K, and  $B_\nu(T)$  is the Planck function; this is referred to as ‘modified blackbody emission’. If those models exactly reflected the properties of emitting sources, then in principle an experiment that had six frequency bands could determine the three emission parameters, as well as the three amplitudes corresponding to that of dust, synchrotron, and the CMB. However, recent observations have shown that neither emission law is universal, that spectral parameters are not necessarily

the same for intensity and polarization and that they vary across the sky [? ? ? ], and thus that the analytic forms and parameter values given above are only approximately valid for averages across the sky [? ]. Also, while both emission laws are well-motivated phenomenological descriptions, the fundamental physics of emissions from grains of different materials, sizes, and temperatures, and of electrons spiraling around magnetic fields implies that these laws are expected to be neither exact, nor universal.

At the low levels of  $r$  targeted by PICO and by other next-decade experiments, even small inaccuracies in foreground modeling and characterization lead to biases and false detections. Several publications have demonstrated that fitting complicated dust temperature profiles using a simple one- or two-temperature model will bias the fitted CMB signal at levels  $\delta r \lesssim 10^{-3}$ , which is significant compared to PICO’s goal [? ? ? ? ].

Further complicating the foreground-separation challenge is the fact that additional polarized foregrounds may exist. Anomalous microwave emission (AME), dust-correlated emission peaking in intensity near 30 GHz, is an important low-frequency foreground in total intensity. It has been tentatively attributed to small, rapidly-spinning dust grains [? ]. Current  $1\sigma$  upper limits on AME polarization are at the level of 1% [? ]. If it is 1% polarized, left uncorrected it would give rise to a bias of  $\delta r \simeq 5 \times 10^{-4}$  [? ]. Astrophysical emission from CO lines at mm wavelengths is expected to be 0.1–1 % polarized [? ? ]. Extragalactic radio sources show a median polarization of 2% [? ? ? ], and there is significant uncertainty about the polarization of dusty galaxies emitting in the PICO wavebands. Initial quantitative estimates show that ignoring radio sources and dusty galaxies may each lead to a bias  $\delta r > 3 \times 10^{-3}$  [? ? ? ] at low and high frequencies, respectively, and ignoring the CO  $J = 1 \rightarrow 0$  line could lead to a bias  $\delta r > 2 \times 10^{-3}$  [? ] at 115 GHz. These levels are appreciable compared to the goals of PICO and other next-decade experiments.

### 0.0.2 Foreground Separation Assessment and Methodology

To investigate the efficacy of PICO in addressing the foreground-separation challenge, we used both an analytic forecast and map-domain simulations.

- **Analytic Forecast** The analytic forecast relies on an established, documented, publicly available, cosmological parameters forecasting code [? ]. The code uses *Planck*-reported Galactic emissions; it assumes that the foreground spectral indices are constant across patch sizes of  $\sim 15^\circ$  on a side; it employs a parametric maximum-likelihood approach<sup>1</sup> to remove the foregrounds and to forecast  $\sigma(r)$ ; and it uses the cleanest 60% of the sky. Lensing  $B$ -modes are included in the input spectra (and are partially removed via delensing, taking into account both noise and foregrounds), but the input for the inflationary signal is  $r = 0$ .

- **Map-Domain Simulations** Map-domain simulations have become the ‘gold standard’ in the community. In this approach, we simulate sky maps that are constrained by available data, but otherwise have a mixture of foreground properties. We ‘observe’ these maps just like a realistic experiment would do, and then apply foreground separation techniques – both parametric and non-parametric<sup>2</sup> – to separate the Galactic and CMB emissions.

To test the results we constructed a variety of full-sky models [? ]. All the models were broadly consistent with available data and with uncertainties from *WMAP* and *Planck*, but they differed in their degrees of Galactic emission complexity. Models included spectral parameters varying spatially and along the line of sight, anomalous microwave emission up to 2% polarized, dust polarization that rotates slightly as a function of frequency because of projection effects, or dust **SED!** (**SED!**)s that depart from a simple modified blackbody. All the foreground maps were generated at native resolution of  $7'$  pixels [? ] with widely-used and thoroughly-tested map-generation codes [? ? ].

For each of the models, we added CMB signals in both intensity and polarization, matching a  $\Lambda$ CDM universe. The input inflationary signal was  $r = 0$ , i.e., no signal, and the  $BB$ -lensing matched the level after

<sup>1</sup>In a parametric approach, foregrounds are assumed to follow emission laws described by a number of free parameters. Parametric models use the frequency dependence of the data in each line of sight to determine the values of the parameters [? ].

<sup>2</sup>Non-parametric techniques rely on the fact that CMB emission is uncorrelated with the foregrounds and thus a correlations analysis within a given spatial/frequency data-cube can be used to separate the two sources of emission [? ? ? ? ].

85% delensing as forecasted for PICO. Each of these sky models had 50 realizations of the PICO noise level. The sky models were analyzed with a variety of foreground separation techniques. Because of limited resources for this study not all models were analyzed with all techniques, and not all realizations were used.

### 0.0.3 Results and Discussion

When using the PICO baseline noise levels with the analytic forecasts we find that  $\sigma(r) = 2 \times 10^{-5}$ , a level that is five times lower than required ( $\sigma(r) = 1 \times 10^{-4}$ , see SO1). We consider this forecast optimistic because it assumes strictly white noise, a specific model for the underlying foregrounds that has only eight parameters<sup>3</sup> per  $15 \times 15 \text{ deg}^2$  pixel, and Gaussian parameter likelihood functions. The foregrounds may be more complex, requiring more parameters (for example, spatially varying temperature for the dust, or more than a single spectral index per source of emission), and may have stronger spatial variations. The parameter likelihoods may not be Gaussian.

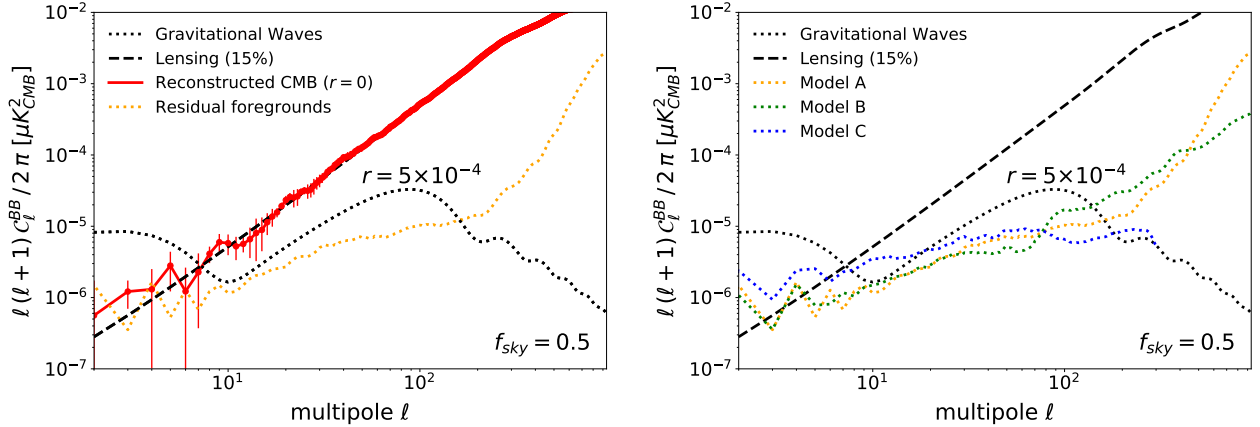


Figure 0.2: Angular power spectra of  $BB$  due to the CMB and of residual foregrounds after an end-to-end map-based foreground-separation exercise. The PICO low noise levels and breadth in frequency coverage enable separation of model A foregrounds such that the residual foreground spectrum (left, yellow dotted) is a factor of ten (four) below a  $BB$  inflationary signal with  $r = 5 \times 10^{-4}$  (black dotted) at  $\ell = 5(80)$ . Within errors, the recovered CMB (red) matches the input CMB, which consists of only lensing  $BB$  (dashed black), over all angular scales  $\ell \gtrsim 6$ . The results for model B are similar (right, green dots); model C, has somewhat higher residuals at low  $\ell$ . In this exercise we used 50% of the sky. Lower foreground residual levels are obtainable with smaller, cleaner patches of  $\sim 10\%$  of sky, which would reduce the residual foregrounds at  $\ell \simeq 80$ .

The ‘gold-standard’ map-based simulations give initial evidence that the combination of PICO’s sensitivity and broad frequency coverage are effective in foreground removal and that PICO will reach the requirement of  $r = 5 \times 10^{-4}$  ( $5\sigma$ ). Fig. 3 shows the results of a foreground-separation exercise over 50% of the sky, with three representative models of Galactic emissions, labeled A, B, and C [? ]. This exercise used GNILC, a non-parametric technique [? ], tuned to give low foregrounds on the largest angular scales, that is, the lowest  $\ell$  modes. The input CMB  $BB$  signal, consisting of only lensing  $B$ -modes, is reconstructed within errors for all  $\ell \gtrsim 5$ . With models A and B the residual foreground  $BB$  power spectrum, encoding the levels of remaining foreground emission after foreground separation is a factor of ten below an inflationary  $BB$  signal for  $r = 5 \times 10^{-4}$  at  $\ell \simeq 4$ . These are the angular scales at which the inflationary signal is stronger than the signal from lensing. Comparing models’ A and B residual foregrounds at this  $\ell$  range to the input  $BB$  foregrounds at, for example, 155 GHz (Fig. ??) we find a strong suppression (a factor of 1000 in temperature), which is a consequence of PICO’s multiplicity of bands and high sensitivity. The residual in model C is a factor of 2 higher than for A and B at  $\ell < 30$ . Of all models, this model is least constrained to match existing sky measurements [? ].

At intermediate angular scales,  $\ell \simeq 80$ , the residual foreground is a factor of four lower than the inflationary signal. We expect lower residuals when GNILC is optimized for this  $\ell$  range; and for reconstructing signals

<sup>3</sup>Six amplitudes for the  $Q$  and  $U$  Stokes parameters of the CMB, dust, and synchrotron emission, and two spectral indices, for dust and synchrotron.

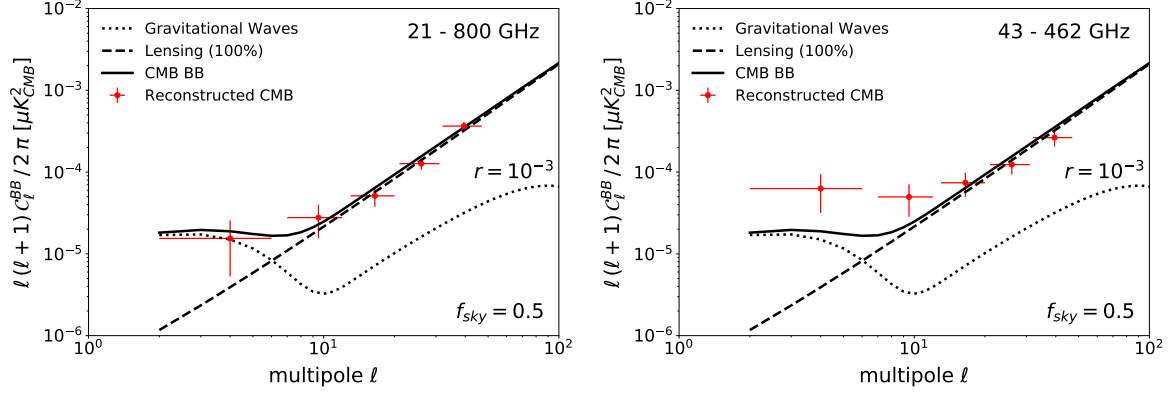


Figure 0.3: **Left:** Foreground separation with all of PICO’s 21 frequency bands recovers the input CMB  $BB$  power spectrum (solid black) without bias (red). The input CMB spectrum has a contribution from lensing (dashed) and an inflationary signal with  $r = 0.001$  (dotted). This exercise uses a parametric approach [?] with foregrounds varying on  $4^\circ$  pixels, and using 50% sky fraction. **Right:** Running the same foreground separation algorithm on the same sky but using only PICO’s bands between 43 and 462 GHz produces an output spectrum (red) that is biased at low multipoles relative to the input. With real data, such a bias would be erroneously interpreted as a higher value of  $r$ .

at this  $\ell$  range, it is sufficient to analyze data from smaller  $\sim 3\%$  regions of the sky. These will have lower mean foreground levels, making the foreground-separation exercise easier, and pushing residuals to levels lower than already demonstrated here for 50% of the sky. With its full-sky coverage, PICO will have access to several independent 3% sky patches, and will thus make several independent measurements of its  $r$  target. Some of our results validate the need for a broad frequency coverage with a strong lever arm on Galactic emissions outside the primary CMB bands. Fig. 2 shows that removing several of PICO’s frequency bands, particularly those that monitor dust at high frequencies and synchrotron at low frequencies, can significantly bias the extracted  $BB$  power spectrum, especially at the lowest multipoles. In this exercise the input CMB contained the lensing signal *and* an inflationary signal with  $r = 0.001$ , and a parametric technique was used for foreground separation [?].

While these results suggest that PICO’s frequency coverage and sensitivity will be adequate for this level of  $r$ , more work should be invested to gain complete confidence. For example, some of the other sky models give a level of residual foregrounds that would give biased measurements reflecting much larger values of  $r$ , even with PICO’s low noise and broad frequency coverage; and some of the foreground-separation techniques appear to give consistently higher foreground residuals than others. To make progress, it is important to continue the simulations and algorithm development program, by running numerous realizations of different sky models and analyzing them with various approaches; optimizing sky masks; and potentially using a combination of techniques to handle large, intermediate, and small angular scale foregrounds differently. It would also be valuable to continue measurements of Galactic emissions with ground- and balloon-based experiments to further reduce the current level of Galactic emission uncertainties.